JOURNAL OF AIRCRAFT
Vol. 42, No. 2, March–April 2005

Propeller Performance at Low Advance Ratio

Ohad Gur* and Aviv Rosen†
Technion—Israel Institute of Technology, 32000 Haifa, Israel

At low advance ratios that are much smaller than the advance ratio where the maximum efficiency of the propeller is obtained, large portions of the blades' cross sections operate at stall conditions. Using two-dimensional nonrotating airfoil data to calculate the propeller's aerodynamic performance at low advance ratios results in large differences between the calculated and measured performance. It turns out that because of rotation the stall characteristics of the airfoil are changed because Coriolis effects delay the boundary-layer separation. Based on previous investigations associated with wind turbines that have been reported in the literature, a simple correction model is presented. It is a straightforward matter to implement this model in existing strip models. The agreement between the calculated and measured results, at low advance ratios, is significantly improved after the introduction of the new model.

Introduction

PROPELLERS are usually designed to operate optimally at a certain design point, for example, the aircraft's cruise conditions. It is clear that propellers also operate at off-design flight conditions that can include takeoff, steep climb, etc. At off-design flight conditions, the efficiency of the propeller drops significantly. To avoid an operation at low efficiencies, propellers are often equipped with variable pitch mechanisms. Yet, there are many aircraft that do not have a variable pitch mechanism because of price, weight, or reliability considerations. These included unmanned aerial vehicles (UAVs), ultralight, and low-priced general aviation aircraft. A fixed-pitch propeller that operates at flight speeds that are much lower than the cruise speeds, namely low advance ratios, suffers from a sharp drop in its efficiency. At low advance ratios, large portions of the blades are operating at stall conditions.

Most of the literature that deals with propellers' performance does not include results for low advance ratios. Evans and Liner[1] present experimental results for propellers at low advance ratios, but they do not present calculated results for these cases. Similar results are also presented in Yaggy and Rogallo.[2] An attempt to use classical methods to calculate the performance of propellers at low advance ratios (advance ratios that are much lower than the advance ratio where maximum efficiency is obtained) exhibits large differences between the calculated and measured thrust, while the same methods exhibit excellent agreement at higher advance ratios. The differences between the calculations and measurements increase as larger portions of the blades experience high cross-sectional angles of attack, beyond the stall limit. Thus, it becomes clear that there are problems in modeling the stall characteristics of cross sections of propellers' blades. It turns out that the measured propeller's thrust is higher (sometimes much higher) than the thrust predicted by calculations where the stall characteristics of a two-dimensional nonrotating airfoil are used.

Himmelskamp[3] was probably the first to investigate the influence of rotation on the stall characteristics of a rotating airfoil. He observed lift coefficients as high as three near the hub of a rotating fan blade. Although it seems to the authors that Himmelskamp's results were not applied in previous analyses of propellers, they were widely used, especially during the last 15 years, in the aerodynamic analysis of wind turbines. The reason is probably the fact that many wind turbines are stall controlled at high wind speeds, and thus their behavior under stalled conditions is very important. Snel[4] presented a detailed analysis of the phenomenon, investigating the boundary layer of a rotating cross section and applying a correction of the airfoil stall characteristics in the analysis of a wind turbine performance. In a later paper[5] Snel et al. presented the use of a simple model to correct the two-dimensional stall characteristics of an airfoil and to account for the rotation effects and compared the results of this model with the experimental results of Bruining et al.[6] Other studies of stall influences on the aerodynamic behavior of wind turbines are presented in several papers.[7–11] The detailed phenomenon is very complicated. Thus, for example, Tangler[11] showed that when strong midspan vorticity exists, it induces a downwash that has a large influence on the local angle of attack of the neighboring cross sections.

In the present paper methods that have been applied previously to describe the influence of rotation on the stall characteristics of wind turbines will be applied to the analysis of propellers operating at low advance rations. The results of the improved theoretical model will be compared with experimental results from the literature.

Theoretical Model

A propeller of diameter D, having b blades and rotating at a frequency n, is considered. The incoming undisturbed flow is axial and has a velocity $\tilde{V}$. (Dimensional velocities are indicated by a tilde above them.) The propeller produces a thrust T and requires a moment Q. The nondimensional advance ratio J, thrust efficient C_T, moment coefficient C_Q, power coefficient C_P, and efficiency η are defined as follows:

$$J = \tilde{V}/(n \cdot D), \qquad C_T = T/(\rho \cdot D^4 \cdot n^2)$$
$$C_Q = Q/(\rho \cdot D^5 \cdot n^2), \qquad C_P = P/(\rho \cdot D^5 \cdot n^3)$$
$$\eta = (C_T \cdot J)/C_P \tag{1}$$

The momentum/blade-element model is one of the commonly used models for the analysis of propellers. It presents a combination of two basic models: the momentum model and the blade-element model.[12]

The momentum model is based on the assumption of an infinitely thin circular actuator disk that allows the fluid to flow through it, but at the same time also allows a pressure jump across it. As shown in Fig. 1, the disc is divided into concentric annuli, and a control volume is defined by the streamlines passing through the boundaries of each annulus.

By using conservation of axial and tangential momentum for each control volume, the following equations are obtained:

$$dC_T = \pi^2/2 \cdot x \cdot (V + F \cdot W_a) \cdot F \cdot W_a \cdot dx \cdot d\Psi$$
$$dC_Q = \pi^2/8 \cdot x^2 \cdot (V + F \cdot W_a) \cdot W_t \cdot dx \cdot d\Psi \tag{2}$$

Received 18 November 2003; revision received 18 April 2004; accepted for publication 21 April 2004.

*Ph.D. Student, Faculty of Aerospace Engineering; ohadg@aerodyne.technion.ac.il.

†Professor, Faculty of Aerospace Engineering; rosen@aerodyne.technion.ac.il. Fellow AIAA.

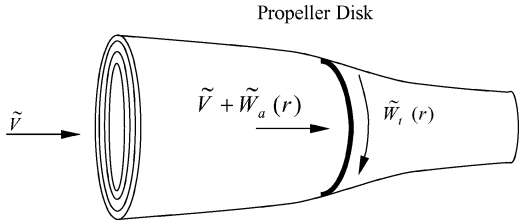

Fig. 1 Control volume of the momentum model.

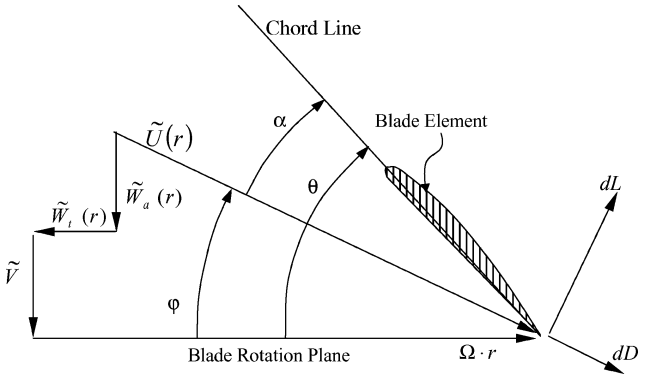

Fig. 2 Blade cross section as used for the blade-element model.

where dC_T and dC_Q are the contributions of the annulus to the thrust and torque coefficients, respectively. V, $W_a(r)$ and $W_t(r)$ are the nondimensional velocity of the undisturbed incoming flow, axial and tangential components of the nondimensional induced velocities through the disk (the last two are functions of the radial coordinate), respectively. Velocities are nondimensionalized after a division by $(\pi \cdot n \cdot D)$, r is the dimensional radial coordinate $(0 \le r \le D/2)$, x is a nondimensional radial coordinate of the disk $(0 \le x \le 1)$, and Ψ is the azimuth angle (0 deg $\le \Psi \le$ 360 deg). F is the tip correction factor, which in the present analysis is calculated according to Goldstein's method.[13]

The blade-element model is based on the assumption that each cross section of a blade behaves like a two-dimensional airfoil. A blade cross section, with all of the velocity components seen by it, is shown in Fig. 2. Ω is the blade angular speed $(\Omega = 2 \cdot \pi \cdot n)$, $\tilde{U}(r)$ is the dimensional cross-sectional resultant velocity, θ is the cross-sectional pitch angle, φ is the cross-sectional incoming flow angle, and α is the cross-sectional angle of attack. If the induced velocity components $[\tilde{W}_a(r), \tilde{W}_t(r)]$ are known and the angle θ is known, then φ and α can be calculated.

Based on the cross-sectional Mach and Reynolds numbers and the angle of attack α, the cross-sectional lift and drag coefficients C_L and C_D are defined. This is done using experimental data or calculations, as presented in the next section.

If the cross-sectional lift and drag coefficients are known, then the lift and drag forces that act on the segment dL and dD, respectively, can be calculated. Based on Fig. 2, it is easily shown that according to the blade-element model

$$dC_T = (b \cdot \pi)/16 \cdot U^2 \cdot c \cdot (C_L \cdot \cos\varphi - C_D \cdot \sin\varphi) \cdot dx \cdot d\Psi$$

$$dC_Q = (b \cdot \pi)/32 \cdot U^2 \cdot c \cdot (C_L \cdot \sin\varphi + C_D \cdot \cos\varphi) \cdot dx \cdot x \cdot d\Psi \tag{3}$$

c is the nondimensional cross-sectional chord.

Equations (2) and (3) form a system of four equations for the four cross-sectional unknowns dC_T, dC_Q, W_a, W_t. The equations are nonlinear in these unknowns, and so they are solved iteratively until convergence.

When the four unknowns have been defined for all of the cross sections, dC_T and dC_Q are integrated along the blade in order to find the thrust and moment coefficients of the propeller.

The momentum/blade-element model presents a very efficient method of calculating the propeller's aerodynamic performance. It requires very small computer resources as compared to detailed vortex models or computational-fluid-dynamic models. The efficiency comes at the price of having to know the two-dimensional airfoil data, namely, $C_L(\alpha, M, Re)$ and $C_D(\alpha, M, Re)$, over a wide range of angles of attack, Mach numbers, and Reynolds numbers.

Two-Dimensional Airfoil Data

A large database for NACA 16 airfoils was built based on available data in the open literature. The main source was Sand et al.,[14] while other sources include similar data[15–16]. The "linear" range is from −4 to 8 deg. Beyond this range, an empirical correction is introduced to represent stall and poststall effects.

For NACA 16 airfoils, there is a lack of data for very large angles of attack. Thus for angles of attack larger than 25 deg, an approximate model was built, which is based on data for a NACA 0012 airfoil for angles of attack at the range −180 to 180 deg.[17]

Look-up tables that depend on the angle of attack and Mach number were built and are used throughout the analysis. Antisymmetric behavior of the lift coefficient for angles of attack larger or smaller than the zero lift angles and a symmetric behavior for the drag coefficient are assumed. A general view of the two-dimensional lift and drag coefficients for large angles of attack, based on Critzos et al.,[17] is shown in Fig. 3.

Himmelskamp[3] was the first to notice the effect of rotation on the stall characteristics of an airfoil. Snel et al.[5] presented an order-of-magnitude analysis of the boundary layer of a rotating airfoil, under stall conditions. After adopting certain simplifications and assumptions, the momentum equation in the circumferential direction ψ becomes[5]

$$\underset{\mathcal{O}\left[\Omega^2 \cdot \tilde{c} \cdot \left(\frac{r}{\tilde{c}}\right)^{\frac{2}{3}}\right]}{\frac{\tilde{V}_\psi \cdot \partial \tilde{V}_\psi}{r \cdot \partial \psi}} \quad \underset{\mathcal{O}\left[\Omega^2 \cdot \tilde{c} \cdot \left(\frac{r}{\tilde{c}}\right)^{\frac{2}{3}}\right]}{+\frac{\tilde{V}_Z \cdot \partial \tilde{V}_\psi}{\partial Z}} = \underset{\mathcal{O}\left[\Omega^2 \cdot \tilde{c} \cdot \left(\frac{r}{\tilde{c}}\right)^{\frac{2}{3}}\right]}{2 \cdot \tilde{V}_r \cdot \Omega} \quad \underset{}{-\frac{\partial P}{\rho \cdot r \cdot \partial \psi}} \quad \underset{\mathcal{O}\left[\frac{\mu}{\rho} \cdot \frac{\Omega^2 \cdot \tilde{c}^{\frac{4}{3}} \cdot r^{\frac{2}{3}}}{\delta^2}\right]}{+\frac{\mu}{\rho} \cdot \frac{\partial^2 \tilde{V}_\psi}{\partial Z^2}} \tag{4}$$

In the upper part of the last equation, the five terms of the equation, two on the left and three on the right side, are presented. $\tilde{V}_\psi$, $\tilde{V}_r$, and $\tilde{V}_Z$ are the radial, circumferential, and axial components of the flow in the boundary-layer region; r, ψ, and Z are the radial, circumferential, and axial coordinates; P is the pressure in the boundary layer; μ is the viscosity; and ρ is the mass density. In the lower part of the last equation, the orders of magnitude of the velocity terms are indicated: δ is the thickness of the boundary layer, Ω is the propeller's angular velocity, r is the local radius of the section, and $\tilde{c}$ is the dimensional chord of the section.

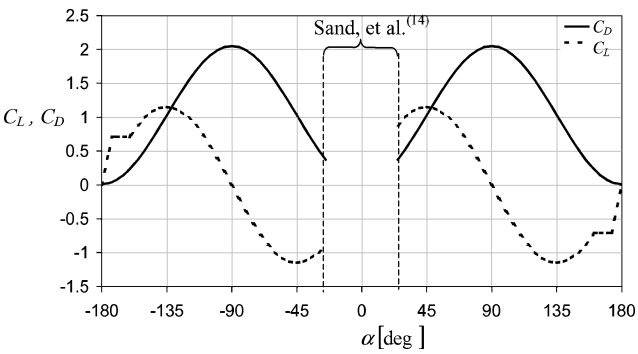

Fig. 3 Two-dimensional lift and drag coefficients for very high angles of attack (based on Critzos et al.[17]).

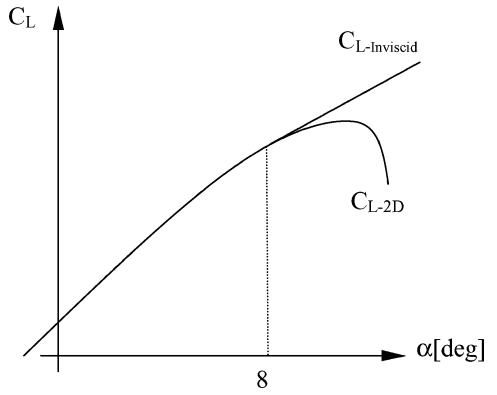

Fig. 4 Inviscid lift coefficient and the two-dimensional one.

The first term on the right side of the equation represents the Coriolis contribution. This contribution appears as a chordwise pressure gradient. The source of this gradient is the radial component of the flow $\tilde{V}_r$ (through the Coriolis effects). This effect delays the separation of the boundary layer and thus delays stall.

By a further use of an ordering scheme analysis, Snel showed that the order of magnitude of the ratio between the radial and circumferential components of the velocity is

$$\tilde{V}_r/\tilde{V}_\psi = \mathcal{O}\left[(r/\tilde{c})^{\frac{1}{3}}\right] \tag{5}$$

It is clearly shown that the parameter $(\tilde{c}/r)$ (or $r/\tilde{c}$) has a major influence on the phenomenon.

Snel et al.[5] proposed a simple correction for the two-dimensional lift coefficient that will also be used in the present analysis. This model assumes two "extreme" cases:

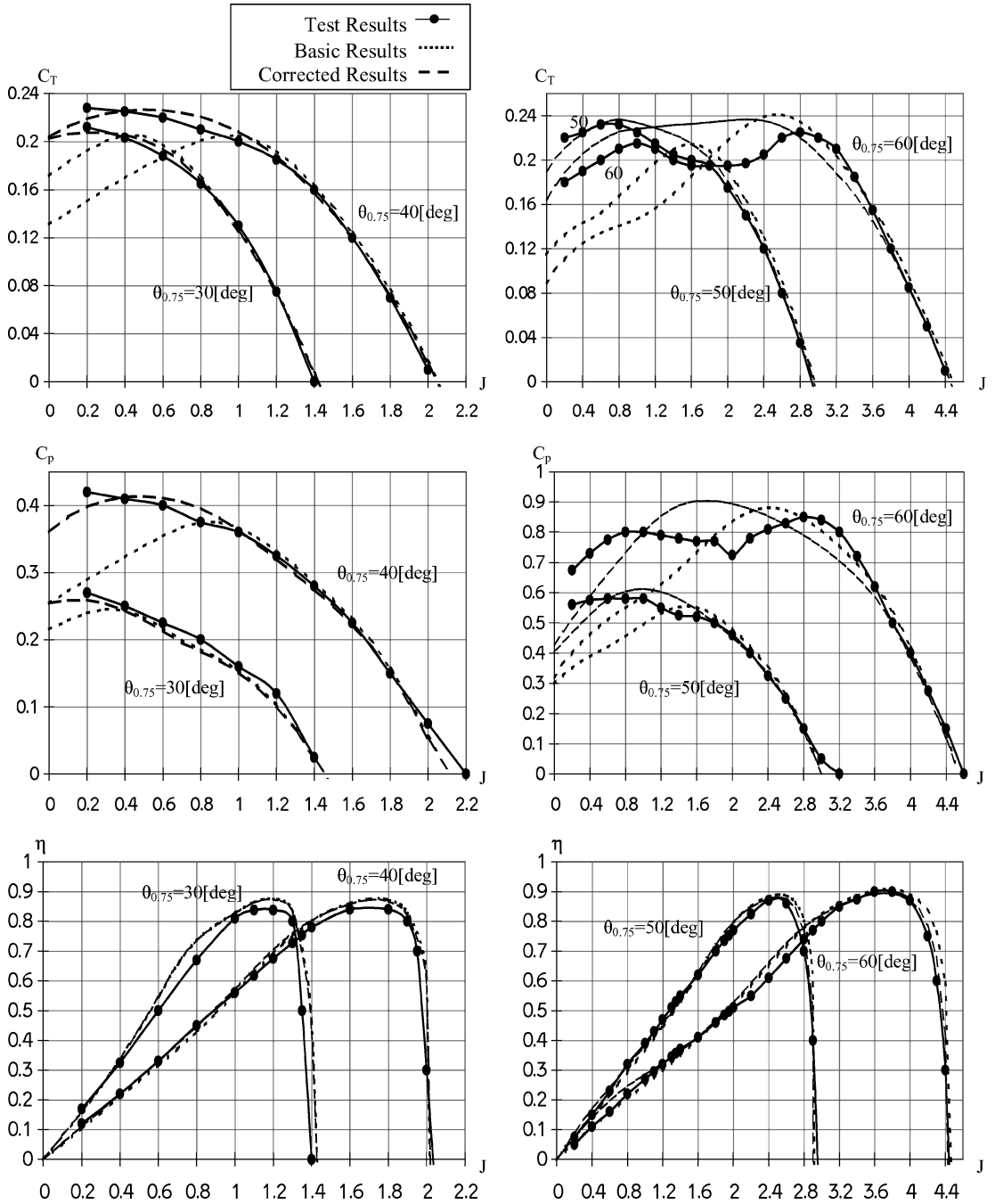

Fig. 5 Thrust, power, and efficiency coefficients, with and without the correction, compared with McLemore and Cannon test results.[18]

1) An inviscid flow where there is no stall and the lift coefficient is a linear function of the angle of attack (shown as $C_{L-\text{inviscid}}$ in Fig. 4).

2) The other case includes the two-dimensional nonrotating viscous case, which is obtained from wind-tunnel tests (shown as C_{L-2D} in Fig. 4).

The three-dimensional model that includes the rotation effects lies somewhere in between these two extreme cases. Thus, the actual three-dimensional lift coefficient that includes rotation effects is described by the following equation:

$$C_{L-3D}(\alpha) = \begin{cases} C_{L-2D}(\alpha) + f(\tilde{c}/r) \cdot |C_{L-\text{Inviscid}}(\alpha) - C_{L-2D}(\alpha)| & \alpha > 8\,\text{deg} \\ C_{L-2D}(\alpha) & 8\,\text{deg} < \alpha < \alpha_{\text{oL}} - 8\,\text{deg} \\ C_{L-2D}(\alpha) - f(\tilde{c}/r) \cdot |C_{L-\text{Inviscid}}(\alpha) - C_{L-2D}(\alpha)| & \tilde{\alpha} < \alpha_{\text{oL}} - 8\,\text{deg} \end{cases} \tag{6}$$

$f(\tilde{c}/r)$ is a function that describes the actual location in between the two extreme cases and, according to Snel's approximation, is a function of the ratio $(\tilde{c}/r)$.

From simple physical reasoning, it is clear that

$$f(\tilde{c}/r) = \begin{cases} 0 & \tilde{c}/r \to 0 \\ 1 & \tilde{c}/r \to \infty \end{cases} \tag{7}$$

It was suggested by Snel to use a hyperbolic tangent as the $f(\tilde{c}/r)$ function, because it poses the characteristics of Eq. (7).

In accordance with the relative increase in the lift coefficient, the drag coefficient is also increased while keeping the ratio between the lift and the drag coefficients unchanged.

Results and Discussion

The case that will be studied first considers a four-bladed propeller having NACA-16 airfoils. This propeller was tested by McLemore and Cannon.[18]

All of the geometric details are given in McLemore and Cannon[18] report. Test results for four different pitch angle settings were presented. (The values that will be indicated in what follows refer to the pitch angles at the $\frac{3}{4}$ radius $\theta_{0.75}$.)

The test results together with the calculations are shown in Fig. 5. Figure 5 presents the thrust coefficient, power coefficient, and efficiency for $\theta_{0.75} = 30$ deg, 40 deg, 50 deg, and $\theta_{0.75} = 60$ deg.

Two kinds of calculated results are shown: basic results that do not include corrections of the lift coefficient for rotation effects on stall and results that include these corrections.

If the calculated results without corrections are compared with the test results, it can be concluded that in general a good agreement is shown at high values of the advance ratio. As the advance ratio is decreased, the differences increase. Table 1 gives the value of the advance ratio, for each pitch angle setting, which is the lower limit for an acceptable agreement between the calculations (that does not include corrections) and the test results. As the blade pitch angle is increased, the value of the advance ratio in Table 1 is increased.

In Tables 2–5 the value of SR_8 is shown for each pitch angle setting, as a function of the advance ratio J. SR_8 is the portion of the disk where the cross-sectional angles of attack are equal or above 8 deg.

As just mentioned, this value (angle of attack equal to 8 deg) indicates the beginning of stall. (This is a representative value because the stall phenomenon is also influenced by the Mach and Reynolds numbers.) Comparison between Tables 1 and 2–5 shows a good correlation between the values of J, where large differences between the calculated results and test results start to show up (Table 1), and values of J where SR_8 starts to increase sharply as J is decreased. This correlation indicates that the disagreement between the basic calculations and the test results is mainly caused by an incorrect description of the stall phenomenon. Therefore, to improve the agreement between the calculated and test results the correction of the two-dimensional airfoil stall characteristics for rotation effects, according to Eq. (6), is introduced.

Table 1 Values of the avance ratio indicating the lower limit of acceptable agreement between calculations that do no include corrections and test results

$\theta_{0.75}$, deg	J
30	0.9
40	1.5
50	1.8
60	3.3

Table 2 Values of SR_8 as functions of the advance ratio J and pitch angle $\theta_{0.75}$:$\theta_{0.75}$ = 30 deg

J	SR_8
0.3	0.468
0.4	0.453
0.5	0.435
0.6	0.406
0.7	0.278
0.8	0.076
0.9	0.019
1.0	0.000
1.1	0.000

Table 3 Values of SR_8 as functions of the advance ratio J and pitch angle $\theta_{0.75}$:$\theta_{0.75}$ = 40 deg

J	SR_8
0.8	0.428
0.9	0.414
1.0	0.388
1.1	0.349
1.3	0.278
1.4	0.193
1.5	0.111
1.6	0.057
1.7	0.000

Table 4 Values of SR_8 as functions of the advance ratio J and pitch angle $\theta_{0.75}$:$\theta_{0.75}$ = 50 deg

J	SR_8
1.6	0.349
1.7	0.304
1.8	0.265
1.9	0.223
2.0	0.162
2.1	0.111
2.2	0.057
2.3	0.019
2.4	0.000

Table 5 Values of SR_8 as functions of the advance ratio J and pitch angle $\theta_{0.75}$:$\theta_{0.75}$ = 60 deg

J	SR_8
2.6	0.265
2.7	0.238
2.8	0.193
2.9	0.162
3.0	0.129
3.1	0.076
3.2	0.057
3.3	0.019
3.4	0.000

The function $f(\tilde{c}/r)$ is chosen as follows:

$$f(\tilde{c}/r) = \tanh\left[P_1 \cdot (\tilde{c}/r)^2 + P_2 \cdot (\tilde{c}/r)\right] \tag{8}$$

The values of the constants P_1 and P_2 are calculated in the following manner: a least-squares matching is carried out between the calculated results and tests results of C_T, for pitch angles 30 deg and 40 deg, along the entire range of advance ratios. As a result of this matching procedure, Eq. (8) becomes

$$f(\tilde{c}/r) = \tanh[7.83 \cdot (\tilde{c}/r)^2 + 9.65 \cdot (\tilde{c}/r)] \tag{9}$$

In Fig. 5 results of the corrected model, where Eq. (9) is used, are also presented. Significant improvement occurs for the low pitch angles (30 deg, 40 deg), where very good agreement between the calculated and measured thrust coefficients is also shown (as opposed to the uncorrected results) for low advance ratios. For the larger pitch angles (50 deg, 60 deg) there is a significant improvement, but the agreement between the thrust coefficients is not as good. The agreement between the calculated and the measured power coefficients is also improved as a result of using Eq. (9), although it is not as good as the improvement in the case of the thrust coefficients. One of the reasons for this is the fact that the power coefficient is influenced by the cross-sectional drag coefficient, which is corrected just to maintain the lift-drag ratio, and not to include any further stall effects.

In the case of the efficiency, there are only very small differences between the basic uncorrected and corrected results, showing good agreement with test results. The reason for that is the fact that the efficiency [see Eq. (1)] is proportional to the ratio between C_T and C_P. Thus, if both C_T and C_P are in error, but the percentage of error in both cases is the same, the ratio still gives the correct value of the efficiency.

It seems that a main reason for the incapability of the present corrected model to give better agreement with the test results at high pitch angles ($\theta_{0.75} = 50$ deg or 60 deg) is the fact that at those pitch angles a large portion of the disk experiences very high cross-sectional angles of attack. Tables 6–9 presents the values of SR_{25} for different settings of pitch angles, as functions of the advance ratio. SR_{25} is the portion of the disk where the cross-sectional angles of attack are equal or larger that 25 deg. It is clearly shown that this parameter increases at high pitch angles. The present model for lift and drag coefficients at very high angles of attack is inaccurate because it is based on test results of a NACA 0012 airfoil at a single Mach number.

In Fig. 6 distributions of the angle of attack along the blade, for a pitch angle of 60 deg, at various advance ratios is shown. For $J = 1$ the crosssectional angles of attack reach values as high as 35 deg.

In Eq. (9), the contribution of the first term [square of $(\tilde{c}/r)$] is very small compared to the second linear term. Therefore, the first term can be neglected, and a linear approximation can be used instead. Using the least-squares procedure that was just described leads to the following expression for the correction function:

$$f(\tilde{c}/r) = \tanh[10.73 \cdot (\tilde{c}/r)] \tag{10}$$

The differences between the results of using Eq. (10) and the results of using Eq. (9) are negligibly small.

Table 6 Values of SR_{25} as functions of the advance ratio J and pitch angle $\theta_{0.75}$:$\theta_{0.75}$ = 30 deg

J	SR_{25}
0.0	0.000
0.1	0.000
0.2	0.000
0.3	0.000
0.4	0.000
0.5	0.000
0.6	0.000
0.7	0.000
0.8	0.000

Table 7 Values of SR_{25} as functions of the advance ratio J and pitch angle $\theta_{0.75}$:$\theta_{0.75}$ = 40 deg

J	SR_{25}
0.0	0.472
0.1	0.264
0.2	0.039
0.3	0.039
0.4	0.020
0.5	0.000
0.6	0.000
0.7	0.000
0.8	0.000

Table 8 Values of SR_{25} as functions of the advance ratio J and pitch angle $\theta_{0.75}$:$\theta_{0.75}$ = 50 deg

J	SR_{25}
0.4	0.421
0.5	0.388
0.6	0.252
0.7	0.146
0.8	0.094
0.9	0.058
1.0	0.020
1.1	0.000
1.2	0.000

Table 9 Values of SR_{25} as functions of the advance ratio J and pitch angle $\theta_{0.75}$:$\theta_{0.75}$ = 60 deg

J	SR_{25}
1.0	0.304
1.1	0.252
1.2	0.194
1.3	0.146
1.4	0.112
1.5	0.058
1.6	0.039
1.7	0.000
1.8	0.000

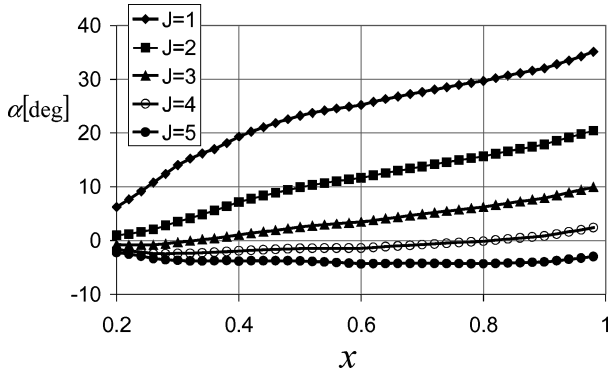

Fig. 6 Angle of attack along the propeller blade at various advance ratio($\theta_{0.75}$ = 65 deg).

To further verify the model, it was used to calculate the performance of another propeller. The propeller that was chosen is the one that was presented by Yaggy and Rogallo.[2] It also has NACA 16 cross sections. The results are shown in Fig. 7.

It seems that there is a problem with the accuracy of the test results of Yaggy and Rogallo.[2] In certain cases the efficiency exceeds unity. Another difficulty is that the report does not give data about the specific values of the propeller rotational speed and tunnel speed, but it only gives the advance ratio that expresses the ratio between both.

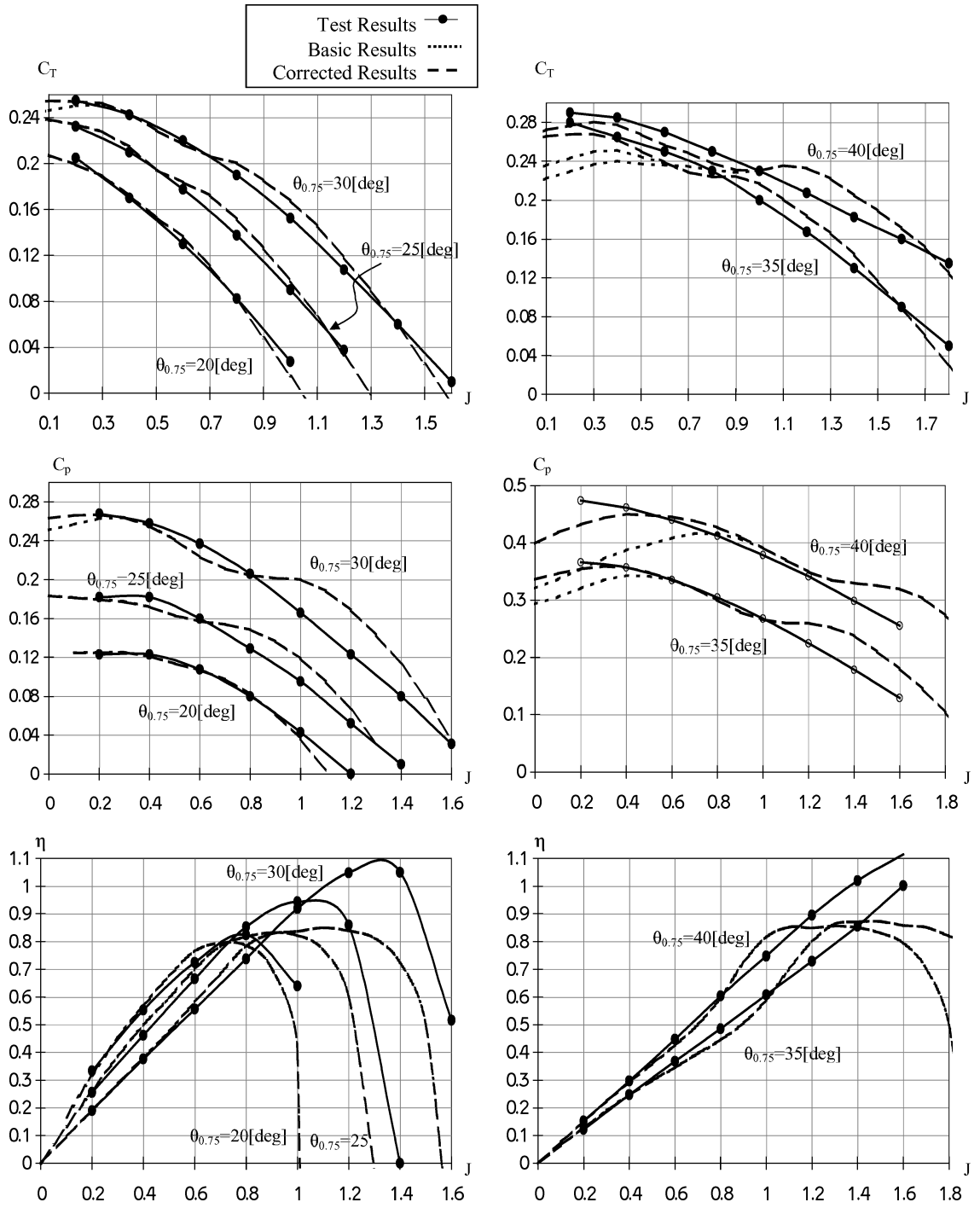

Fig. 7 Thrust, power, and efficiency coefficients, with and without the correction, compared with Yaggy and Rogallo test results.[2]

In spite of the problems with the test results, it is shown that by using the correction of Eq. (10) (without carrying a least-squares matching procedure for the tests of Yaggy and Rogallo[2]) there is an improvement in the agreement between the calculated and test results at low advance ratios, especially for $\theta_{0.75} = 35$ deg and 40 deg. Yet, in these results the influence of stall is much smaller than the previous case.[18]

Conclusions

Fixed-pitch propellers are widely used in UAVs and ultralight and general aviation aircraft. When these propellers are operating at low advance ratios, namely, advance ratios that are much lower than the advance ratio where the maximum efficiency is obtained, large portions of the blade's cross sections experience angles of attack that exceed stall. When the performance of the propellers operating at these conditions are calculated by any blade-element method using two-dimensional nonrotating airfoil data, the results of the analysis show large differences when compared with test data. It turns out that because of Coriolis effects, associated with the rotation and the radial component of the velocity, the boundary-layer separation is delayed, and thus stall is delayed.

The present analysis is based on a momentum/blade-element method. Like other blade-element models, this method is very efficient and requires relatively small computer resources as compared to detailed vortex models or computational-fluid-dynamics models. The efficiency comes at the price of a need for a very large database of airfoil characteristics over a wide range of angles of attack, Mach numbers, and Reynolds numbers. The problem

of organizing such a database becomes the main difficulty of applying the method. These data are usually based on wind-tunnel tests that are expensive to perform and time consuming.

In the present paper, a simple model of correcting the two dimensional nonrotating airfoil data to account for rotation effects has been presented. This model is based on previous analyses of wind turbines operating at stall conditions. The model includes unknown constants that are determined after applying a least-squares procedure of matching between calculated results and test data. This correction model is probably a function of the specific airfoil, Mach number of the cross-sectional flow, and speed of rotation. Yet it was shown that a correction model that was obtained for a certain propeller also gave good results for another propeller that uses the same airfoils.

When the correction model is used, the agreement between the calculations and test results is significantly improved. The agreement is usually better in the case of the thrust coefficient than in the case of the power coefficient. This agreement deteriorates when the angles of attack become extremely large (over 25 deg).

References

[1]Evans, A. J., and Liner, G., "A Wind Tunnel Investigation of the Aerodynamic Characteristics of a Full-Scale Sweptback Propeller and Two Related Straight Propellers," NACA RM-L50J05, Jan. 1951.

[2]Yaggy, F. P., and Rogallo, L. V., "A Wind Tunnel Investigation of Three Propellers Through an Angle of Attack Range from 0° to 85°," NASA TN-D-318, May 1960.

[3]Himmelskamp, H., "Profile Investigations on Rotating Airscrew," Ph.D. Dissertation, Gottingen Univ., Göttingen, Germany, 1945.

[4]Snel, H. R., "Scaling Laws for the Boundary Layer Flow on Rotating Wind Turbine Blades," *Proceedings of the Fourth IEA Symposium on the Aerodynamics of Wind Turbines*, ETSU-N-118, Dept. of Energy, U.K., Jan. 1991.

[5]Snel, H. R., Houwink, R., and Bosschers, J., "Sectional Prediction of Lift Coefficients on Rotating Wind Turbine in Blades in Stall," Rept. C93-052, Energieonderzoek Centrum Nederland, Petten, The Netherland, Dec. 1994.

[6]Bruining, A., van Bussel, G. J. W., Corten, G. P., and Timmer, W. A., "Pressure Distribution from a Wind Turbine Blade; Field Measurement Compared to Two-Dimensional Wind Tunnel Data," Inst. for Wind Energy, Delft Univ. of Technology, Rept. IW-93065R, The Netherlands, Aug. 1993.

[7]Hamed, A., Herring, J., and Povinelli, L., "Three-Dimensional Flow Phenomena in Fluid Machinery," Fluids Engineering Symposia Series, Vol. FED-32, American Society of Mechanical Engineering, New York, 1985, pp. 121–132.

[8]Sorensen, J. N., "Prediction of Three-Dimensional Stall on Wind Turbine Blade Using Three-Level, Viscous-Inviscid Interaction Model," *European Wind Energy Association Conference and Exhibition*, European Wind Energy Association, Oct. 1986, pp. 429–435.

[9]Ronsten, G., "Static Pressure Measurements on a Rotating and a Non-Rotating 2.375 m Wind Turbine Blade. Comparison with 2D Calculations," *Journal of Wind Engineering and Industrial Aerodynamics*, Vol. 39, No. 1, 1992, pp. 105–118.

[10]Tangler, J. L., and Selig, M. S., "Evaluation of an Empirical Model for Stall Delay due to Rotation of HAWTS," National Renewable Energy Lab., Rept. CP-440-23258, Golden, CO, June 1997.

[11]Tangler, L. J., "Insight into a Wind Turbine Stall and Post-Stall Aerodynamics," WindPower 2003, May 2003.

[12]Durand, W. F., *Aerodynamic Theory*, Vol. IV, Dover, New York, 1943, Chap. V.

[13]Goldstein, S., "On the Vortex Theory of Screw Propellers," *Proceedings of the Royal Society of London*, Series A., Vol. 123, No. 792, 1929, pp. 440–495.

[14]Sand, E., Elliot, A., Jr., and Borst, H. V., "Summary of Propeller Design Procedures and Data, Vol. 3, Hub, Actuator and Control Designs," U.S. Army Air Mobility Research and Development Lab., Technical Rept. 73-34C, Dept. of the Army, Fort Eustis, VA, Nov. 1973.

[15]Lindsey, W. F., Stevenson, D. B., and Baley, B. N., "Aerodynamic Characteristics of 24 NACA 16—Series Airfoils at Mach Numbers Between 0.3 and 0.8," NACA TN-1546, Sept. 1948.

[16]Maksymiuk, C. M., and Watson, S. A., "A Computer Program for Estimating the Aerodynamic Characteristics of NACA 16—Series Airfoils," NASA TM-85696, Sept. 1983.

[17]Critzos, C. C., Heyson, H. H., and Boswinkle, R. W., "Aerodynamic Characteristics of NACA 0012 Airfoil Section at Angles of Attack From 0° to 180°," NACA TN-3361, Jan. 1955.

[18]McLemore, H. C., and Cannon, M. D., "Aerodynamic Investigation of Four-Blade Propeller Operating Through an Angle of Attack Range from 0° to 180°," NACA TN-3228, June 1954.